

RESEARCH ARTICLE

Identification of differential gene expression patterns in human arteries from patients with chronic kidney disease

Jane Stubbe,^{1,6} Vibe Skov,² Helle Charlotte Thieson,³ Karl Egon Larsen,⁴ Maria L. Hansen,⁴ Boye L. Jensen,¹ Bente Jespersen,⁵ and Lars M. Rasmussen⁶

¹Cardiovascular and Renal Research Unit, Institute of Molecular Medicine, University of Southern Denmark, Odense, Denmark; ²Department of Hematology, Zealand University Hospital, Roskilde, Denmark; ³Department of Nephrology, Odense University Hospital, Odense, Denmark; ⁴Department of Cardiothoracic and Vascular Surgery, Odense University Hospital, Odense, Denmark; ⁵Department of Nephrology, Aarhus University Hospital, Aarhus, Denmark; and ⁶Center for Individualized Medicine in Arterial Diseases, Department of Clinical Biochemistry and Pharmacology, Odense University Hospital, Odense, Denmark

Submitted 22 August 2017; accepted in final form 7 February 2018

Stubbe J, Skov V, Thieson HC, Larsen KE, Hansen ML, Jensen BL, Jespersen B, Rasmussen LM. Identification of differential gene expression patterns in human arteries from patients with chronic kidney disease. *Am J Physiol Renal Physiol* 314: F1117–F1128, 2018. First published February 7, 2018; doi:10.1152/ajprenal.00418.2017.—Uremia accelerates atherosclerosis, but little is known about affected pathways in human vasculature. This study aimed to identify differentially expressed arterial transcripts in patients with chronic kidney disease (CKD). Global mRNA expression was estimated by microarray hybridization in iliac arteries ($n = 14$) from renal transplant recipients and compared with renal arteries from healthy living kidney donors ($n = 19$) in *study 1*. *Study 2* compared nonatherosclerotic internal mammary arteries (IMA) from five patients with elevated plasma creatinine levels and age- and sex-matched controls with normal creatinine levels. Western blotting and immunohistochemistry for selected proteins were performed on a subset of *study 1* samples. Fifteen gene transcripts were significantly different between the two groups in *study 1* [fold changes (FC) > 1.05 and false discovery rates (FDR) < 0.005]. Most upregulated mRNAs associated with cellular signaling, apoptosis, TNF α /NF- κ B signaling, smooth muscle contraction, and 10 other pathways were significantly affected. To focus attention on genes from genuine vascular cells, which dominate in IMA, concordant deregulated genes in *studies 1* and *2* were examined and included 23 downregulated and eight upregulated transcripts (settings in *study 1*: FC > 1.05 and FDR < 0.05; *study 2*: FC > 1.2 and $P < 0.2$). Selected deregulated gene products were investigated at the protein level, and whereas HIF3 α confirmed mRNA upregulation, vimentin showed upregulation in contrast to the mRNA results. We conclude that arteries from CKD patients display change in relatively few sets of genes. Many were related to differentiated vascular smooth muscle cell phenotype. These identified genes may contribute to understanding the development of arterial injury among patients with CKD.

atherosclerosis; calcification; uremia; vascular remodeling

INTRODUCTION

Chronic kidney disease (CKD) is associated with markedly augmented cardiovascular morbidity and overall mortality (6),

partly due to occlusive arterial disease (30, 45). In addition to atherosclerosis, arterial features of uremia include calcification of tunica media, which is caused by uremic substances and hyperphosphatemia (14). This results in decreased vascular compliance, increased pulse-wave velocity, and ultimately left ventricular hypertrophy and heart failure (16, 23, 34). The initial media calcification in uremia occurs along the elastic fibers and the internal elastic lamina and is not typically associated with inflammation (37, 47). Medial vascular smooth muscle cells may transdifferentiate as a response to stress or injury from the contractile phenotype into osteoblast-like or chondrocyte-like cells (29, 33, 36, 42), which is a likely initial step in extracellular matrix calcification that eventually leads to cardiovascular events (51, 54). This is in contrast to intimal calcification within atherosclerotic lesions that is associated with inflammation and necrotic cores (15). The mediators of accelerated and uremia-associated arterial disease are unknown. Experimental murine models with 5/6 nephrectomy on an apolipoprotein E^{-/-} background and in uremic rats identified dysregulated gene transcripts involved in vascular smooth muscle cell structure, inflammation, and extracellular matrix remodeling (4, 43). These rodent models are far from the human setting, and whether similar gene expression patterns are found in the vascular wall in human uremic patients remains to be elucidated. The present study was designed to test the hypothesis that uremia is associated with dysregulated gene expression patterns across human arterial beds, particularly of gene products associated with vascular smooth muscle differentiation, calcification, and matrix alterations. Our approach was transcriptomic array investigation of gene expression differences between 14 human iliac arterial samples from kidney-engrafted CKD patients and 19 renal artery samples from healthy kidney donors (*study 1*). These tissue samples are dominated by various degrees of atherosclerosis, and to focus the resulting list of identified uremia-related gene transcripts potentially from plaques to changes in vascular cells, i.e., mostly smooth muscle cells, *study 2* was included. In this part, internal mammary arteries from patients with normal and elevated plasma creatinine levels were compared. These arteries are homogenous, nonatherosclerotic “repair” arteries obtained from coronary by-pass operations (40). The combined

Address for reprint requests and other correspondence: J. Stubbe, Dept. of Cardiovascular and Renal Research, Institute of Molecular Medicine, Univ. of Southern Denmark, J. B. Winsloevej 21, 3. 5000 Odense, Denmark (e-mail: jstubbe@health.sdu.dk).

results include a series of transcripts, which represent changes in similarly sized systemic conduit arteries among patients with decreased kidney function. A selection of these gene products was further investigated at the protein level.

METHODS

Populations. *Study 1* was a comparison of human iliac artery samples collected from 18 renal transplant recipients (RTR) undergoing elective renal transplantation (plasma creatinine range: 574–1,272 $\mu\text{mol/l}$), with 23 renal arterial samples obtained from living donors undergoing nephrectomy. All kidney donors had a normal plasma creatinine level (range: 50–111 $\mu\text{mol/l}$) and glomerular filtration rate (GFR; $>80 \text{ ml/min} \cdot 1.73 \text{ m}^2$ measured by Cr^{51} -EDTA clearance). One donor sample was obtained from a deceased donor. All samples were collected in accordance with ethics approval from the Den Videnskabetiske Komite for Region Syddanmark (no. S-20070059). All artery samples were not cleaned off the adventitial layer, and thus the attempt was to maintain all layers intact in tissue samples used for analysis. Four RTR samples and four control donor samples were excluded due to low or very poor RNA quality. Clinical parameters obtained from patient files of the patients included in the microarray analyses (19 controls and 14 RTRs) are shown in Table 1. Cause of renal failure within the included RTRs was glomerulonephritis (57%), diabetic nephropathy (7%), autosomal dominant polycystic kidney disease (7%), and end-stage renal disease of unknown cause (29%). In *study 2*, material from five internal mammary artery (IMA) samples was obtained from our biobank, as previously described (40). Sampling was approved by the Den Videnskabetiske Komite for Region Syddanmark (no. S-20100044). The five IMA samples were from patients with elevated plasma creatinine levels (range: 158–941 $\mu\text{mol/l}$); four patients were chronic hemodialysis patients, and one patient had the adrenals and pituitary gland removed 28 yr ago and thus received hormonal replacement therapy. Five IMA samples from age- and sex-matched individuals with no known renal disease and normal plasma creatinine levels (range: 78–100 $\mu\text{mol/l}$) were collected and used as controls. Clinical parameters from *study 2* are

shown in Table 1. At the time of collection, arterial samples were cut in two, where one sample was snap-frozen in liquid nitrogen for RNA and protein isolation and the other fixed in neutral formalin and then embedded in paraffin for histological analyses.

RNA sample preparation. Total RNA were isolated from all artery samples using the 5-ml TRIzol reagent (Sigma-Aldrich) isolation method, as previously described (49). Quantity of RNA was measured using the NanoDrop spectrophotometer ND-8000 (NanoDrop Technologies), and RNA integrity was assessed using the Agilent 2100 Bioanalyzer (Agilent Technologies, Palo Alto, CA).

Amplified RNA preparation and microarray hybridization. The MessageAMP TM III amplification kit (Ambion, Austin, TX) was used to amplify and fragment 300 ng of total RNA to biotin-labeled aRNA, which was hybridized to Affymetrix HG-U133A 2.0 chips (Affymetrix, Santa Clara, CA) as previously described (49).

Data treatment and statistical analysis. Initial array data analysis was done using the affymetrix package (www.bioconductor.org) implemented in the statistical programming language R (20). The robust multiarray average method was used to perform background correction, normalization, and gene expression index calculation (21). Only perfect match probes were used for data analysis. Differences in gene expression between groups were calculated for each gene using the regularized *t*-test limma (50), and the Benjamini-Hochberg method [false discovery rate (FDR)] was used as correction for multiple hypothesis testing (3) to judge differences. To further minimize the false-positive deregulated gene transcripts, Bonferroni correction was applied. The low number of observations in *study 2* made *lege artis* corrected *P* values difficult to achieve; however, the combination of genes with a *P* value of <0.2 and fold change (FC) of ≥ 1.2 from *study 2* with genes in *study 1* with FDR of <0.05 and FC of ≥ 1.2 was used operationally to yield an enriched group of genes, which better represented genuine vascular cell genes, associated with CKD. All data are available from Gene Expression Omnibus (accession no. GSE38752; <http://www.ncbi.nlm.nih.gov/geo/>).

Global pathway analysis. Gene Map Annotator and Pathway Profiler (GenMAPP 2.1) (9) together with its accessory program Microarray Pathway Profiles (MAPP) Finder 2.1 (12) were used to assess

Table 1. Clinical data for the study population

	CKD Patients (Set 1)			Internal Mammary Arteries (Set 2)		
	Donors	Renal transplant recipients	<i>P</i> value	Controls	Elevated plasma creatinine	<i>P</i> value
Sex (male/female)	8/11	9/5		4/1	4/1	
Age, yr	50.1 \pm 2.3	40.3 \pm 3	$P < 0.02$	63.1 \pm 4.4	62.8 \pm 4.9	
Years with known renal disease		10.8 \pm 2.2				
Body mass index, kg/m ²	27.6 \pm 1.1 (8)	26.2 \pm 1.2 (8)		27.7 \pm 3.4 (3)	23.0 \pm 0.2 (4)	
Systolic blood pressure, mmHg	131 \pm 3 (18)	155 \pm 7 (13)	$P < 0.01$	133 \pm 18	143 \pm 12 (4)	
Diastolic blood pressure, mmHg	78 \pm 2 (18)	93 \pm 4 (13)		80 \pm 6	83 \pm 13 (4)	
Plasma creatinine, μM	80 \pm 4 (18)	858 \pm 53	$P < 0.0001$	88 \pm 4	530 \pm 133	$P < 0.03$
Hb A _{1c} , %	5.4 \pm 0.8 (15)	5.7 \pm 0.4 (11)		6.0 \pm 0.4	6.2 \pm 0.4 (4)	
P-cholesterol (mM)	4.9 \pm 0.3 (15)	4.4 \pm 0.5 (11)		3.9 \pm 0.5	4.2 \pm 0.6 (4)	
P-cholesterol LDL (mM)	2.7 \pm 0.2 (15)	2.3 \pm 0.3 (11)		2.2 \pm 0.3	2.4 \pm 0.6 (4)	
P-cholesterol HDL (mM)	1.5 \pm 0.1 (15)	1.0 \pm 0.1 (11)	$P < 0.002$	1.2 \pm 0.1	1.1 \pm 0.1 (4)	
P-triglyceride (mM)	1.7 \pm 0.3 (15)	2.9 \pm 0.6 (11)		1.6 \pm 0.2	1.9 \pm 0.4 (4)	
B-leucocyte ($\times 10^9/\text{ml}$)	7.5 \pm 0.6 (15)	8.5 \pm 0.6 (11)		ND	ND	
Smoking (yes/no/not available)	9/3/6	5/2/7		3/2/0	0/5/0	
Other medications						
β -Blockers		54%		80%	60%	
Diuretics		36%		20%	80%	
Aspirin		18%		80%	80%	
Ang II receptor antagonists/ACE inhibitors		45%		0%	20%	
Statins		18%		100%	80%	
Calcium antagonists		45%		40%	40%	

CKD, chronic kidney disease; ND, not determined; Ang II, angiotensin II. Other diseases: 1 renal transplant recipient also had insulin-dependent diabetes mellitus. One included donor artery was obtained from a deceased donor, and thus clinical parameters not included in this table. Internal mammary artery group: One of the controls suffers from disseminated sclerosis.

significantly regulated pathways in *data set 1*. A total of 192 pathways were applied to the data. A z -score of >2.0 was used as criteria for significantly regulated pathways.

Protein isolation and Western blots. Proteins from the arteries were isolated from the phenol phase used for RNA isolation according to the manufacturer's instructions. Protein pellets were resuspended in 1% SDS buffer (300 mM sucrose, 25 mM imidazole, and 1 mM EDTA, pH7.2) with complete protease inhibitor cocktail (Roche Diagnostics) overnight at 50°C. In five control iliac artery samples and 10 RTR artery samples the protein yield was too low to be used for Western blotting. An equal amount of proteins were separated on a 5–16% SDS-PAGE-gel (Invitrogen) and blotted on a PVDF membrane. Primary antibodies against vimentin (1:1,000 DAKO) or hypoxia-inducible factor-3 α (HIF-3 α) (1:1,000, Abcam) were applied, followed by incubation with appropriate horseradish peroxidase (HRP)-conjugated secondary antibody (1:2,000), and visualized using the HCL chemiluminescent kit (Bio-Rad) and exposed on film (Kodak). As equal loading and “housekeeping” biological control, stripped membranes were incubated with primary antibody directed against β -actin (1:20,000; Abcam). Protein band density was semiquantified using Gel Doc 2000, quantity one (version 4.6.3; Bio-Rad). Statistical analysis was done by unpaired t -test using prism 6.0. $P < 0.05$ was considered significantly different.

Immunohistochemistry. Five-micrometer artery sections from donor controls ($n = 12$) and renal transplant recipients ($n = 11$) from *data set 1* were deparaffinized, demasked in citrate buffer (DAKO), and incubated overnight with the following primary antibodies: vimentin (1:200; DAKO), HIF-3 α (1:50; Abcam) or CD68 (1:200; Abcam), and α -actin (1:500; cy3-labeled, Abcam). Appropriate HRP-conjugated secondary antibody (1:1,000; DAKO) was applied for 45 min, positive staining was identified with DAKO's DAB solution, and then sections were counterstained with hematoxylin or DAPI. In addition, sections were stained with Masson-trichrome (Sigma-Aldrich), Verhoeff-van Gieson (Atom Scientific), and Alizarin red S (Merck Milipore).

RESULTS

Patient characteristics. In *study 1* (RTR iliac arteries vs. control renal arteries), the patient groups were of mixed sex (64% males vs. 42% males; Table 1, *set 1*), and RTRs were significantly younger and had higher systolic blood pressure, plasma creatinine concentration, and plasma B-leukocyte count, whereas circulating HDL concentration was significantly lower compared with the control group (Table 1, *set 1*).

The RTRs had on average suffered from renal disease for 10 yr (range 1–35 yr) and were treated with peritoneal dialysis or hemodialysis, except for two predialysis patients, both suffering from focal segmental glomerulosclerosis with plasma creatinine levels of 856 and 877 $\mu\text{mol/l}$, respectively. Two renal transplant recipients had previously received a renal transplantation. All RTRs were before transplantation treated pharmacologically by combinations of β -blockers, diuretics, aspirin, angiotensin-converting enzyme (ACE) inhibitors/angiotensin II receptor antagonists, calcium channel blockers, and statins, as indicated in Table 1, *set 1*. Some of the controls were on various medications not related to arterial or renal disease. One donor received an ACE inhibitor (enalapril) and thiazide, and another donor received prednisolone and methotrexat for psoriasis arthritis. In *study 2*, with IMA samples, the groups were matched with respect to sex, age, and plasma cholesterol concentrations, hemoglobin A_{1c} (HbA_{1c}), and blood pressure (Table 1, *set 2*).

CKD-associated transcriptome patterns in human arteries. In *study 1* of arteries from renal transplant recipients versus healthy donor controls, analysis of transcript abundances revealed that a total of 3,523 of 22,278 genes were differentially expressed when judged with an uncorrected t -test-calculated P value of <0.05 . When corrected for multiple hypothesis testing, using the false discovery rate (FDR) method with a FDR of <0.05 , 325 genes showed significantly differential expression. To further minimize the number of false-positive deregulated gene transcripts, Bonferroni correction was applied. As shown in Table 2, 15 genes displayed a fold change (FC) of >1.05 and a FDR of <0.005 and corrected by Bonferroni when data from the RTR group was compared with the healthy donor controls. Of these, 11 gene products were significantly downregulated (Table 2), whereas growth-associated protein 43 showed the largest difference when FC was considered (20% of control). Also of note is that prostacyclin synthase mRNA and the extracellular matrix protein periostin was downregulated (approximately one-third of control). By contrast, four gene products displayed significantly elevated levels in the RTR-iliac arteries with these criteria (Table 2). The most upregulated gene transcripts were the transcription factor homeobox C10 (~ 3 -fold) and tumor-associated calcium signal

Table 2. Microarray output of the top 15 deregulated gene expression in RTR iliac arteries vs. renal arteries from donor controls

Gene ID	Gene Name	FC	P Value	FDR
PITX1	Paired-like homeodomain 1	2.1	9.4E-09	0.0001
GAP43	Growth-associated protein 43	−5.1	1.1E-08	0.0001
HOXC10	Homeobox C10	2.9	5.4E-08	0.0004
FOXD1	Forkhead box D1	−2.5	6.8E-08	0.0004
POSTN	Periostin, osteoblast specific factor	−2.7	2.8E-07	0.001
EMP2	Epithelial membrane protein 2	−1.4	3.3E-07	0.001
PTGIS	Prostaglandin I ₂ (prostacyclin) synthase	−1.6	4.2E-07	0.001
ARHGAP26	Rho GTPase activating protein 26	1.6	6.6E-07	0.002
MPPED2	Metallophosphoesterase domain containing 2	−2.5	8.8E-07	0.002
AKR1C2	Aldo-keto reductase family 1, member C2	−1.8	9.0E-07	0.002
PTH1H	Parathyroid hormone-like hormone	−2.1	1.4E-06	0.003
ANKRD6	Ankyrin repeat domain 6	−2.3	1.9E-06	0.003
LRRC17	Leucine-rich repeat containing 17	−2.5	2.0E-06	0.003
TACSTD2	Tumor-associated calcium signal transducer 2	2.4	2.1E-06	0.003
VIM	Vimentin	−1.4	3.5E-06	0.004

RTR, renal transplant recipient; FC, Fold change; FDR, false discovery rate.

Table 3. Top 12 most downregulated pathways in RTR arteries analyzed with MAPPFinder 2.0

MAPP Name	Changed (n)	Measured (n)	On MAPP (n)	%Changed	z-Score	Permute P Value
Hs_aminosugars_metabolism	11	32	54	34.4	4.2	0.001
Hs_D_glutamine_and_D_glutamate_metabolism	3	4	14	75	4.1	0.004
Nucleotide_sugars_metabolism	5	12	36	41.7	3.4	0.003
Glycogen_metabolism	10	35	36	28.6	3.3	0.001
Smooth_muscle_contraction	28	144	156	19.4	3.2	0.006
Glycosaminoglycan_degradation	5	14	17	35.7	2.9	0.01
Riboflavin_metabolism	4	10	21	40	2.9	0.01
α 6/ β -Integrin_NetPath_1	14	66	67	21.2	2.6	0.01
Ribosomal_proteins	17	88	88	19.3	2.4	0.02
Wnt_NetPath_8	19	104	110	18.3	2.3	0.01
TGF- β -receptor_NetPath_7	25	146	151	17.1	2.3	0.03
Synthesis_and_degradation_of_ketone_bodies_KEGG	2	5	5	40	2.0	0.1
Prostaglandin_synthesis_regulation	7	31	31	22.6	2.0	0.05

MAPP, microarray pathway profiles. Pathways with a z -score of ≥ 2.0 are shown. A P value of <0.05 and a FC of up to -1.05 were used as criteria for gene expression changes in RTR iliac arteries vs. donor control renal arteries. The z -score is based on $n = 3,935$ genes linked to a MAPP and $r = 440$ distinct genes meeting the criteria for change in expression. Changed (n): no. of genes changed. Measured (n): no. of genes measured on the chip. On MAPP (n): no. of genes on the MAPP. %Changed: changed (n)/measured (n).

transducer 2 (2.4 fold; Table 2). With the use of GenMAPP and MAPPfinder, 12 pathways were significantly downregulated (z -score ≥ 2.0 ; Table 3). The most downregulated pathway was amino sugar metabolism (z -score = 4.2) and the smooth muscle contraction signaling pathway (z -score = 3.3; Table 3). In addition, 10 pathways were significantly upregulated (z -score ≥ 2 , Table 4), with the most upregulated pathways aminoacyl tRNA biosynthesis (z -score = 3.3) and the apoptosis pathway and the proinflammatory IL-6, IL-7, and TNF α /NF- κ B pathways (Table 4).

In study 2, internal mammary arteries from patients with elevated plasma creatinine were compared with age- and sex-matched controls with normal plasma creatinine (530 ± 133 vs. $88 \pm 4 \mu\text{mol/l}$; $n = 5$ in each group; Table 1). This artery is typically free of atherosclerosis (40). Four-hundred seventy-four gene transcripts were significantly expressed when judged with an uncorrected t -test-calculated P value of <0.05 . However, no transcripts from the internal mammary arteries were significantly different between patients with elevated plasma creatinine levels and patients with no known kidney disease when correcting for multiple testing. When the list of changed gene transcripts was studied, the seemingly most changed transcripts were inter- α -trypsin inhibitor heavy chain H4 (3 times higher than non CKD), *PRRC2C* proline-rich coiled-coil 2C (BAT2L2), the anti-proliferative family protein Tob2, and

the transcription regulator bromodomain containing 2 (BRD2) (data not shown). The protease inhibitor cystatin C, a circulating marker of kidney injury (10, 26), was lowered to one-third in mammary arteries from patients with elevated plasma creatinine levels, and epithelial membrane protein 3 was twofold downregulated.

Common CKD gene expression patterns across arterial beds. The results from study 1 display *lege artis* statistically significantly expressed genes between CKD and non-CKD arterial tissue with various degrees of atherosclerotic lesions. However, to narrow this finding to genes related to genuine vascular cells, genes were combined from the two data sets with the following setting: RNAs, which in comparisons between groups displayed a FC of ≥ 1.2 and FDR of <0.05 in study 1 using strict statistical methods and were combined with a loose cutoff $P < 0.2$ and FC ≥ 1.2 in the IMA group (study 2). This extracted 23 gene transcripts, which were congruently downregulated (Table 5), and eight gene transcripts, which were congruently upregulated (Table 6). Among the downregulated genes, two were associated with smooth muscle cell contraction (MYO1D and CALM1), and four gene products were involved in cell adhesion (CD9, DPT, IGFBP7, and CRTAC1). Moreover, the filament protein, vimentin, associated with the differentiated state of mesenchymal cells, the proteoglycan fibromodulin, important for collagen fibril archi-

Table 4. Top 10 most upregulated pathways in RTR arteries analyzed by MAPP Finder 2.0

MAPP Name	Changed (n)	Measured (n)	On MAPP (n)	%Changed	z-Score	Permute P
Aminoacyl tRNA biosynthesis	8	22	24	36.4	3.3	0.006
Glycine serine and threonine metabolism	10	32	64	31.3	3.1	0.004
IL-7 NetPath 19	12	44	44	27.3	2.8	0.01
IL-6 NetPath 18	22	98	100	22.4	2.8	0.007
Cyanoamino acid metabolism	3	6	22	50.0	2.7	0.04
Apoptosis	18	82	82	22.0	2.4	0.02
TNF α /NF- κ B NetPath 9	33	176	187	18.8	2.3	0.02
Sphingophospholipid biosynthesis	2	4	10	50.0	2.2	0.09
Phospholipid degradation	6	21	30	28.6	2.1	0.047
Triacylglyceride synthesis BiGCaT	6	21	24	28.6	2.1	0.047

Pathways with a z -score of ≥ 2.0 are shown. A P value of <0.05 and a FC of up to -1.05 were used as criteria for gene expression changes in RTR iliac arteries vs. donor control renal arteries. The z -score is based on $n = 3,935$ genes linked to a MAPP and $r = 514$ distinct genes meeting the criteria for change in expression. Changed (n): no. of genes changed. Measured (n): no. of genes measured on the chip. On MAPP (n): no. of genes on the MAPP. %Changed: changed (n)/measured (n).

Table 5. *Congruently downregulated gene transcripts in both the RTR vs. donor control arteries and in mammary arteries from patients with elevated plasma creatinine levels vs. age- and sex-matched control mammary arteries*

Description (Symbol)	RTR vs. Donor Arteries Study			Mammary Arteries From By-Pass Patients With Elevated Creatinine Levels And Age- and Sex-Matched Controls	
	FC	P value	FDR	FC	P value
Retinoic acid receptor responder (tazarotene induced) 1 (RARRES1)	-2.5	2.6E-04	0.03	-1.7	0.12
Cartilage acidic protein 1 (CRTAC1)	-2.0	3.4E-05	0.01	-1.5	0.14
Dermatopontin (DPT)	-2.0	6.7E-04	0.05	-1.5	0.08
Left-right determination factor 2 (LEFTY2)	-1.7	6.0E-05	0.01	-1.3	0.12
Myosin ID (MYO1D)	-1.7	4.7E-04	0.04	-2.1	0.20
Retinol binding protein 1, cellular (RBP1)	-1.7	2.3E-05	0.009	-1.5	0.11
Fibromodulin (FMOD)	-1.7	5.6E-06	0.005	-1.3	0.10
CD9 molecule (CD9)	-1.7	7.3E-05	0.02	-1.9	0.18
Homeobox B7 (HOXB7)	-1.6	1.6E-05	0.008	-1.6	0.04
Microfibrillar-associated protein 4 (MFAP4)	-1.5	1.3E-04	0.02	-1.9	0.04
Dishevelled associated activator of morphogenesis 2 (DAAM2)	-1.4	4.7E-05	0.01	-1.5	0.11
Vimentin (VIM)	-1.4	3.5E-06	0.004	-1.8	0.08
Calmodulin 1 (phosphorylase kinase, δ) (CALM1)	-1.4	3.1E-04	0.03	-1.6	0.16
Fasciculation and elongation protein zeta 1 (zyglin I) (FEZ1)	-1.4	1.9E-04	0.03	-1.4	0.15
RAB6A, member RAS oncogene family (RAB6A)	-1.3	7.8E-05	0.02	-1.4	0.16
Diazepam binding inhibitor (GABA receptor modulator, acyl-coenzyme A binding protein) (DBI)	-1.3	9.3E-05	0.02	-1.7	0.07
Rac/Cdc42 guanine nucleotide exchange factor (GEF) 6 (ARHGEF6)	-1.3	5.6E-04	0.04	-1.6	0.04
Insulin-like growth factor binding protein 7 (IGFBP7)	-1.3	3.9E-04	0.04	-1.5	0.11
Septin 8 (39692)	-1.3	4.8E-04	0.04	-1.3	0.10
GNAS complex locus (GNAS)	-1.3	1.0E-04	0.02	-1.7	0.04
SMT3 suppressor of mif two 3 homolog 3 (S. cerevisiae) (SUMO3)	-1.2	1.5E-04	0.02	-1.5	0.09
Adenosine kinase (ADK)	-1.2	2.8E-04	0.03	-1.4	0.03

texture (52), the elastin-related innate immune system protein MFAP4 (44), and DAAM2, a modulator of wnt receptor complex (25), were congruently downregulated in both studies. Among the upregulated gene transcripts, four mRNAs were identified to be associated with the apoptosis and ubiquitin protein degradation pathway (RAB40A, CFLAR, RBBP6, and PSME4), and two genes were identified as transcription factors [HIF-3 α , transcription factor A, mitochondrial (TFAM)]. Also, the potassium channel (KCNB1) was congruently significantly upregulated in both studies.

Morphological comparison of the arteries. The control renal arteries exhibited a slightly larger cross-sectional area compared with the iliac arteries, and there were no obvious changes

in elastin arrangement, collagen deposition, or media thickness between renal transplant recipient iliac arteries and renal artery controls (Fig. 1). In the RTR arteries in *study 1*, Alizarin red staining revealed discrete foci with calcifications in the media layer of the RTR arteries, which were not seen in the control arteries (Fig. 1). Also, infiltration of macrophages (CD68) was present in the RTR arteries, whereas only few CD68-positive cells were detected in the control arteries (Fig. 1).

Effect of CKD on abundance and localization of selected proteins in arterial tissue. HIF3 α -mRNA displayed congruent upregulation in CKD in *studies 1* and 2 (Table 6), and putative differences were analyzed at the protein level. By immunohistochemical labeling, HIF3 α was associated with vascular

Table 6. *Congruently upregulated gene transcripts in both the RTR vs. donor control arteries and in mammary arteries from patients with elevated plasma creatinine levels vs. age- and sex-matched control mammary arteries*

Description (Symbol)	RTR vs. Donor Arteries Study			Mammary Arteries From By-Pass Patients With Elevated Plasma Creatinine Levels And Age- and Sex-Matched Controls	
	FC	P value	FDR	FC	P value
Potassium voltage-gated channel, Shab-related subfamily, member 1 (KCNB1)	1.7	2.58E-04	0.03	1.3	0.1
Hypoxia inducible factor 3, α -subunit (HIF3A)	1.6	2.99E-05	0.01	1.3	0.12
NOP56 ribonucleoprotein homolog (yeast) (NOP56)	1.5	2.13E-05	0.008	1.4	0.12
Proteasome (prosome, macropain) activator subunit 4 (PSME4)	1.4	2.48E-05	0.009	1.3	0.13
RAB40A, member RAS oncogene family (RAB40A)	1.4	3.79E-04	0.04	1.4	0.12
Retinoblastoma binding protein 6 (RBBP6)	1.3	1.15E-04	0.02	1.5	0.16
CASP8 and FADD-like apoptosis regulator (CFLAR)	1.2	3.55E-04	0.04	1.2	0.17
Transcription factor A, mitochondrial (TFAM)	1.2	6.92E-04	0.048	1.2	0.16

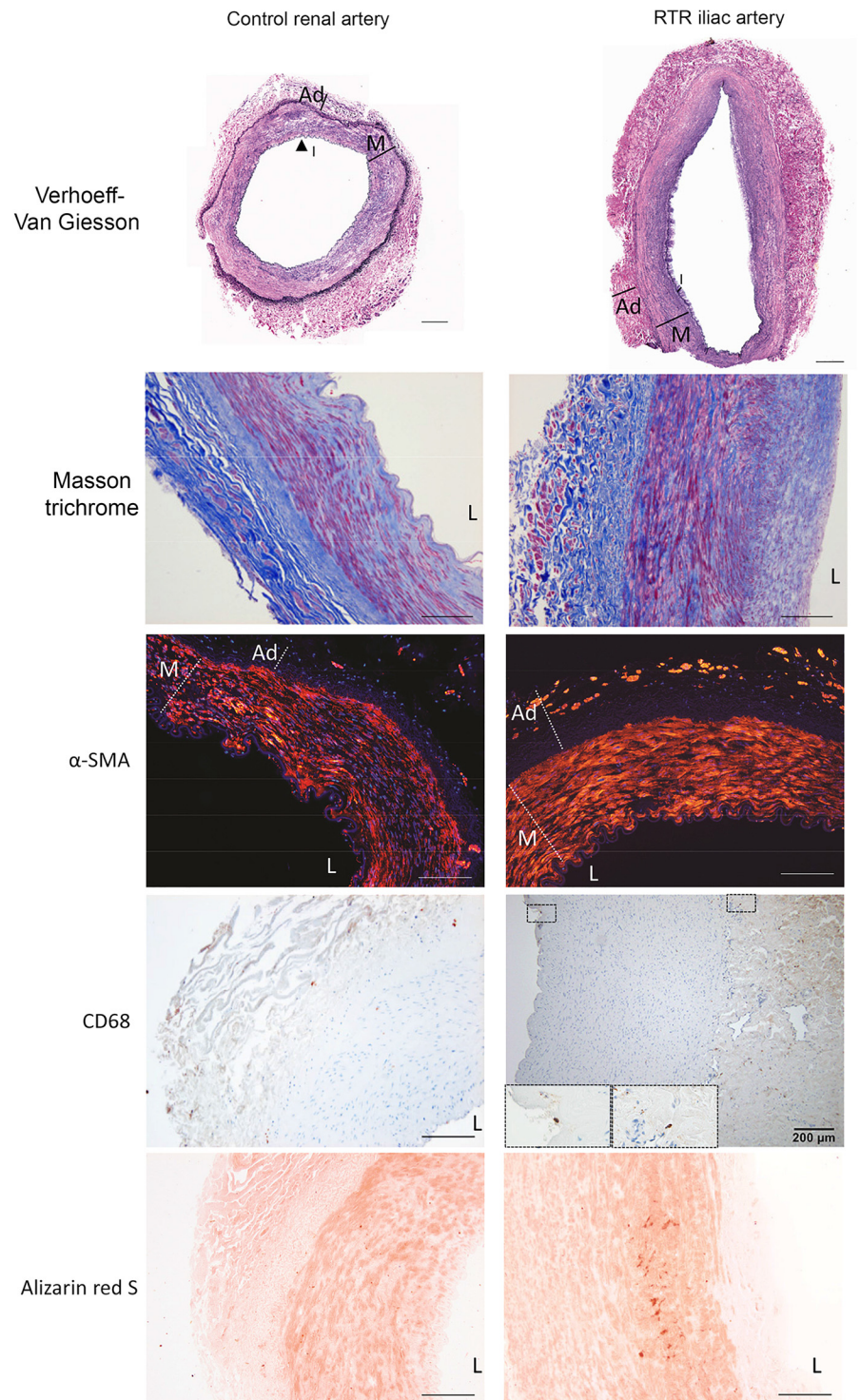
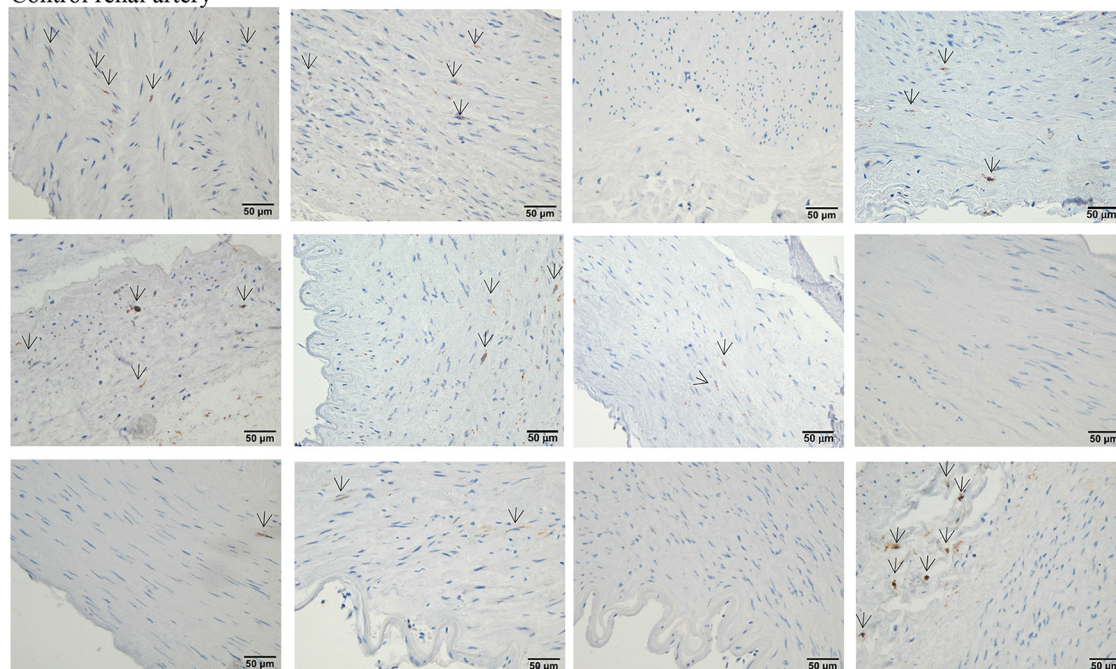


Fig. 1. Artery characteristics. In control renal arteries and renal transplant recipient (RTR) iliac arteries, elastin fibers were identified with Verhoeff van Gieson black staining. The staining also revealed that iliac and renal arteries were of same size and had the same relative layer composition. Collagen deposition was identified by Masson trichrome, where collagen fibrils appear blue. Vascular smooth muscle cells were identified by immunofluorescence labeling of α -smooth muscle actin (α -SMA)-positive cells (red). No major difference in smooth muscle cell distribution or layers was uncovered. Infiltration of CD68-positive cell macrophages was likely observed in the adventitial layer. Boxes indicate enlargements of micrographs inserted in the corner. Alizarin red was used to identify calcifications and showed Alizarin red-positive staining in a few places in the media layer of the RTR arteries ($n = 11-12$). I, intima; M, media; Ad, adventitia. Scale bars, 200 μ m, except for Verhoeff-Van Gieson, where the scale bar is 500 μ m.

smooth muscle cells. All analyzed RTR samples contained some HIF3 α -positive cells predominately associated with vascular smooth muscle cells. When HIF3 α -positive cells were grouped in high/intermediate/low abundance on the specimens, three showed high abundance, and six had intermediate abundance of the 11 patient samples analyzed ($n = 11-12$; Fig. 2). In contrast, in the control donor renal artery samples no labeling or only a few positive cells were detected in four out of 12 specimens, and only some HIF3 α -positive cells associ-

ated with vascular smooth muscle cells were seen in the remaining eight specimens ($P = 0.05$, Freeman-Halton-Fisher exact test; figure 2 and 3A). A trend toward higher extractable amounts was in addition observed by Western blot analysis ($P = 0.28$; Fig. 3B). Vimentin mRNA levels showed congruent downregulation in CKD arteries (Tables 2 and 5), and at the protein level, vimentin immunolabeling was associated with vascular smooth muscle cells in media and endothelial cells of vasa vasorum of both control and RTR arteries, with no

Control renal artery



RTR iliac artery

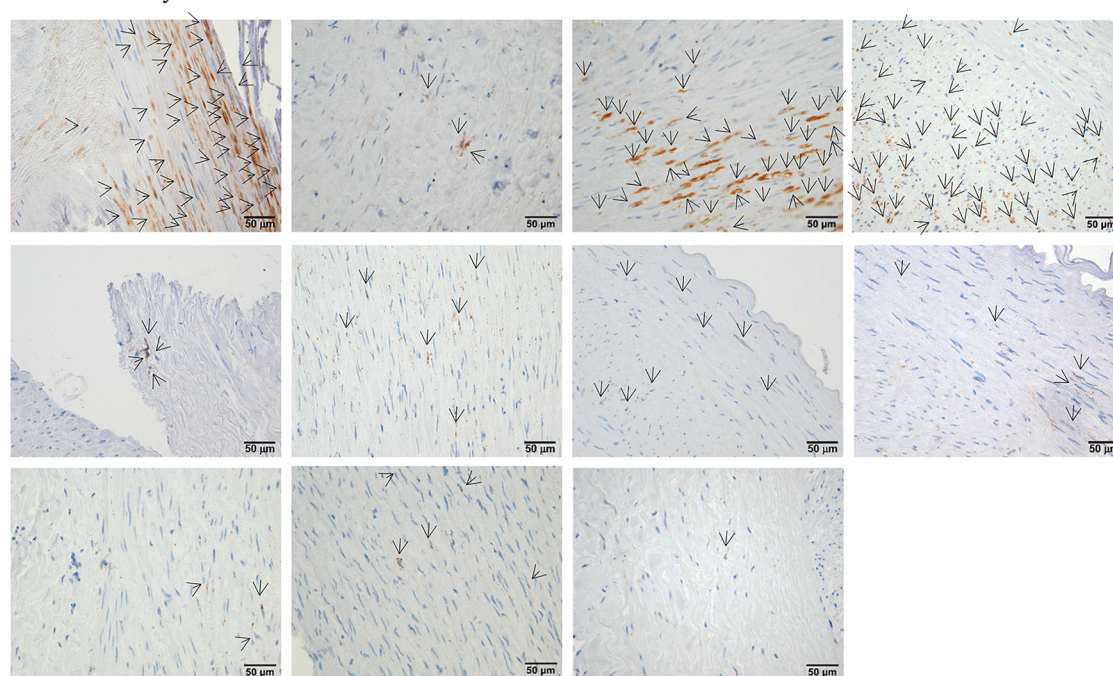


Fig. 2. Hypoxia-inducible factor-3 α (HIF-3 α) protein distribution. HIF-3 α -positive cells were localized predominantly to a few vascular smooth muscle cells in both RTR iliac arteries and control renal arteries ($n = 11$ – 12). Four of 12 donor control renal artery samples were HIF-3 α -negative or HIF-3 α was detected only in a single cell, whereas the other 8 displayed discrete staining in a few cells. All RTR samples contained HIF-3 α -positive cells, with high abundance in 3 out of 11 samples. Arrowheads point to HIF-3 α -positive cells.

obvious differences between the vascular distributions (Fig. 4A). However, by Western blot analysis, vimentin was slightly but significantly upregulated in the RTR arteries (Fig. 4B), which was the opposite of the RNA array result (Table 2 and 5).

DISCUSSION

The present study was designed to identify common gene expression pattern changes in human conduit arteries associ-

ated with CKD. CKD is a marked accelerator of vascular disease. The approach was to investigate global gene transcript abundances in human arteries from RTR patients and compare them with control arteries from donors with no renal disease. To gain information on the pattern of changes across conduit arteries and to detect early changes, a parallel study with internal mammary arteries from patients with renal impairment was performed. Despite the relative small group sizes in study

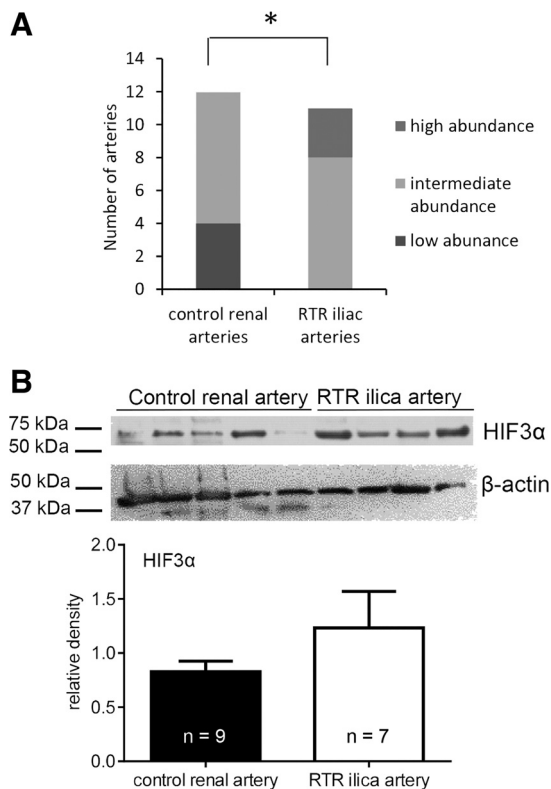


Fig. 3. HIF-3 α protein abundance. **A**: scoring of the HIF-3 α immunohistochemical labeling in high abundance and intermediate abundance (some HIF-3 α -positive cells) or low HIF-3 α -positive cells from the patients displayed in Fig. 2 revealed a significant difference in HIF-3 α tissue distribution between RTR artery samples and control iliac samples; $n = 11$ – 12 , when Freeman-Halton-Fisher exact test was used. $*P = 0.05$. **B**: representative Western blot identified HIF-3 α protein bands in all tested artery samples that migrated at the expected size of 60 kDa. Densitometric analysis did not detect any statistically significant difference in relative HIF-3 α protein levels between arteries from the RTR and control groups ($n = 7$ – 9).

1, 15 gene transcripts were significantly different when very conservative statistical tests were applied with corrections for multiple testing. The most downregulated gene transcript was growth-associated protein 43, which is a calcium-sensitive membrane-bound phosphoprotein involved in neuron sprouting during axon genesis and regeneration (46, 48). Prostacyclin synthase was downregulated, and prostacyclin is cardioprotective, and anti-inflammatory and prostacyclin analogs attenuate renal functional decline (24, 56). Periostin was reduced to one-third in uremia. This is in contrast to recently published data showing a threefold upregulation of periostin in uremic rat aortas (43). Periostin is an extracellular matrix protein known to be involved in vascular smooth muscle cell migration through integrin interactions (27) and matrix metalloprotease production (17), thus contributing to vascular remodeling. The discrepancy between the present findings and those in the uremic rat aorta may be the difference in anatomic origin in our study, or it could be associated with the timespan of the disease or patient medication or simply be species dependent. The most upregulated gene transcript was homeobox C10, which was involved in fat distribution and adipocyte function. Homeobox C10 in adipocytes was positively correlated to BMI (5). No difference in BMI was observed between groups in our study. Perivascular fat and connective tissue were not quanti-

fied in the present study. The tumor-associated calcium signal transducer 2 was increased in RTR arteries. It is highly expressed on the surface of invasive cells, e.g., trophoblast and tumor cells (32), it is involved in angiogenesis, and it is affected by changes in plasma calcium, and thus it could contribute to accelerated artery injury in CKD patients. The gene product parathyroid hormone-like hormone (PTHrP) was significantly downregulated. This gene regulates endochondral bone development by effects on cellular differentiation and calcium ion transport. It is regulated by vitamin D and may be involved in calcification programs (19). It has been suggested to be involved in vascular calcification among hemodialysis patients (31).

We identified several dysregulated pathways in RTR arteries, and among those, the smooth muscle cell contraction pathway was downregulated, which was completely in line with the expected vascular smooth muscle cell phenotypic switch in CKD patients (29, 33, 36, 42). The apoptosis pathway and several proinflammatory pathways of IL-6, IL-7, and TNF α were upregulated in the RTR arteries, which is in accord with acceleration of the atherosclerotic process that includes proinflammatory mechanisms and accelerated apoptosis. The sphingophospholipid biosynthesis pathway was upregulated and may contribute to the proatherosclerotic stage, as sphingosine-1-phosphate (S1P) has been shown to modulate inflammation and angiogenesis (59). To focus the list of regulated genes from *study 1* to molecules, which are related to genuine vascular cells, i.e., to avoid differences related to atherosclerotic plaque-associated changes, *study 2* compared internal mammary arteries obtained from patients with normal and elevated plasma creatinine levels. The internal mammary artery does not develop atherosclerosis (40). Post hoc analysis, when conservative statistical testings in *study 1* and a loose cutoff $P < 0.2$ in *study 2* were applied, displayed a list of 23 gene transcripts congruently downregulated and eight gene transcripts congruently upregulated. Although these genes are not selected after *lege artis* statistical principles and false-positive molecules may occur, it is likely that this group of selected genes is associated with the effects of kidney impairment in vascular cells. This interpretation fits with the identification of the selected genes that were related to vascular smooth muscle biology, such as, e.g., IGFBP7, which binds insulin-like growth factors (IGF-1 and IGF-2) and is an adhesion protein known to be involved in tumor vessel stabilization by promoting smooth muscle cell recruitment and differentiation (38). It is also a known inducer of G1 cell arrest, and, together with tissue inhibitor of metalloproteinases-2, it has been identified as a potent urinary biomarker of acute kidney injury induced by sepsis, shock, major surgery, and trauma (22). Thus, downregulation of IGFBP7 in CKD arteries may allow cell proliferation. The cytoskeletal filamentous protein vimentin is stimulated by TGF β 1 and TNF α and induces vascular smooth muscle cell migration (28, 57), suggesting a role in the atherogenic process. Vimentin gene transcript was congruently downregulated in the two data sets, where also the TGF β and TNF α pathways were downregulated in the RTR arteries. At the protein levels, vimentin was associated with the majority of vascular smooth muscle cells and some endothelial cells in both groups. In contrast to the RNA data, vimentin protein levels were significantly elevated in RTR arteries. This is in agreement with an *in vitro* study showing that vimentin

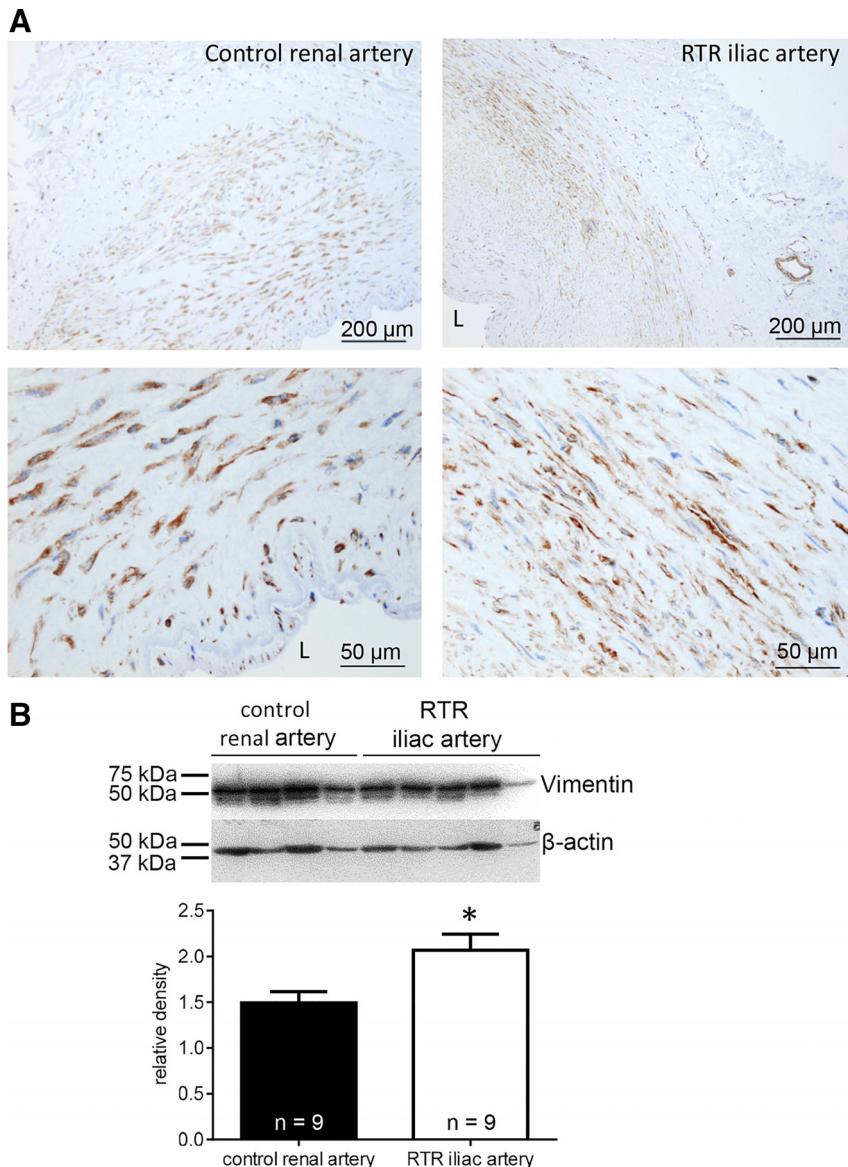


Fig. 4. Vimentin protein distribution and abundance. **A**: vimentin immunoreactivity in RTR iliac arteries and control renal arteries was widely abundant in vascular smooth muscle cells and was localized in the cytosol of most vascular smooth muscle cells in all samples analyzed. There was no obvious difference in the distribution of vimentin between RTR iliac artery samples and control renal arteries ($n = 11$ – 12). **B**: Blots show representative Western blotting experiments for vimentin and β -actin. Vimentin-positive bands migrated at the expected molecular size of 57 kDa and were detected in both RTR and control arteries. Densitometric analysis showed that the relative vimentin levels were significantly upregulated in RTR arteries ($n = 9$). *Significance, $P < 0.05$ by Student's t -test.

was upregulated in endothelial cells exposed to uremic serum (7). This discrepancy between microarray results and protein levels is a common observation (55). Protein levels do not only reflect mRNA levels but are also influenced by protein turnover rates, and it can be speculated that opposite changes could represent compensatory downregulation of mRNA due to low protein turnover.

The expression of HIF3 α was congruently upregulated in both arterial beds in CKD patients, and at protein level, HIF3 α -positive cells were predominately vascular smooth muscle cells and were more abundant in specimens from RTR patients. HIF complexes consist of an unstable oxygen-sensing α -subunit (1–3) and a stable β -subunit. HIF-1 α is upregulated by oxidized LDL and is essential for macrophage survival and promotes atherosclerosis (39, 60). HIF-1 α and HIF-2 α are expressed in proinflammatory M1 macrophages and anti-inflammatory M2 macrophages, respectively, and affect nitric oxide production in opposite directions (53) and may contribute to changes in systemic arterial pressure (8). Less is known

about function of HIF-3 α . It is believed to be a negative regulator of HIF-1 α and HIF-2 α by competing for the common β -subunit (18). Thus HIF-3 α may fine-tune the HIF response in its target tissue and could dampen the proatherogenic response induced by HIF-1 α . In the present study, HIF-3 α protein was localized in few vascular smooth muscle cells. This is in line with previous observations where HIF-3 α was upregulated in endothelial and vascular smooth muscle cells in hypoxic conditions (1). Overexpression of HIF-3 α decreased the expression of VEGFA (1). Thus the presence of HIF-3 α might limit vascular smooth muscle cell proliferation. Several other gene transcripts (PSME4, CFLAR, RAB40A, and RBBP6) involved in cell metabolism were congruently upregulated in both studies. An augmented proteasome activity has previously been reported in uremic rabbits, and inhibition of proteasome or NF- κ B prevented the accelerated atherosclerosis in uremia (13). In support of this, inhibition of proteasome activity prevented platelet-dependent arterial thrombosis induced in renovascular hypertensive rats (35). Also, in vitro

experimental data show that the ubiquitin-proteasome pathway is augmented in vascular smooth muscle cells exposed to uremic serum (58). It is well established that uremic patients often suffer from enhanced skeletal muscle wasting caused by augmented protein turnover. The increased protein degradation is partly mediated via upregulation of the ubiquitin-proteasome pathway and perhaps mediated by metabolic acidosis (2, 41). Thus, it is likely that upregulation of this pathway also leads to vascular muscle cell wasting in humans, as seen in the experimental models, and thus contributes to the accelerated atherogenesis and matrix accumulation in CKD patients.

There are limitations to the present study: The cross-sectional design allows us only to generate hypotheses and does not provide mechanistic information. Moreover, the small sample size is a drawback ($n = 14$ – 19 patients in *study 1* and $5 + 5$ in *study 2*), as is the different medication (e.g. with and without immunosuppression). However, the human tissue approach is the first one, to our knowledge. Insisting on a human approach, the RTR artery samples and control arteries in *study 1* were from different vascular beds, but both were conduit arteries and the morphological analysis showed similar artery size and structure (Fig. 1) in accord with a comparable elastin content (11). This limitation was addressed experimentally in *study 2*, where age and sex matching was also possible. Data in *study 2* were interpreted with a “loose” P value, and it cannot be excluded that the identified genes may be falsely positive findings. However, the approach provides a quite narrow identification of an altered gene expression profile related to vascular cells and not invasive bone marrow-derived hematopoietic cells. In conclusion, the present study provides a first human map of altered gene expression and pathways in CKD associated with the arterial wall. The limited number of relevant genes will allow a test of functional importance at the physiological level.

ACKNOWLEDGMENTS

We thank Ann Sofie Madsen, Inger Nissen, and Susanne Hansen for skillful technical assistance.

GRANTS

This project was supported by the A. P. Møller Foundation, the Helen and Ejnar Bjørnøw Foundation, the Danish Society of Nephrology Research Fond, the Alfred Madsen and Spouse foundation, and the Waagens Fond.

DISCLOSURES

No conflicts of interest, financial or otherwise, are declared by the authors.

AUTHOR CONTRIBUTIONS

J.S., V.S., H.C.T., K.E.L., B.L.J., B.J., and L.M.R. conceived and designed research; J.S., V.S., H.C.T., K.E.L., and M.L.H. performed experiments; J.S., V.S., and L.M.R. analyzed data; J.S., V.S., B.L.J., and L.M.R. interpreted results of experiments; J.S. prepared figures; J.S., B.L.J., and L.M.R. drafted manuscript; J.S., V.S., H.C.T., K.E.L., M.L.H., B.L.J., B.J., and L.M.R. edited and revised manuscript; J.S., V.S., H.C.T., K.E.L., M.L.H., B.L.J., B.J., and L.M.R. approved final version of manuscript.

REFERENCES

- Augstein A, Poitz DM, Braun-Dullaeus RC, Strasser RH, Schmeisser A. Cell-specific and hypoxia-dependent regulation of human HIF-3 α : inhibition of the expression of HIF target genes in vascular cells. *Cell Mol Life Sci* 68: 2627–2642, 2011. doi:10.1007/s00018-010-0575-4.
- Bailey JL, Price SR, England BK, Jurkovitz C, Wang X, Ding X, Mitch WE. Signals regulating accelerated muscle protein catabolism in uremia. *Miner Electrolyte Metab* 23: 198–200, 1997.
- Benjamini Y, Hochberg Y. Controlling the false discovery rate: a practical and powerful approach to multiple testing. *J R Stat Soc B* 57: 289–300, 1995.
- Bro S, Borup R, Andersen CB, Moeller F, Olgaard K, Nielsen LB. Uremia-specific effects in the arterial media during development of uremic atherosclerosis in apolipoprotein E-deficient mice. *Arterioscler Thromb Vasc Biol* 26: 570–575, 2006. doi:10.1161/01.ATV.0000201060.47945.cb.
- Brune JE, Kern M, Kunath A, Flehmig G, Schön MR, Lohmann T, Dressler M, Dietrich A, Fasshauer M, Kovacs P, Stumvoll M, Blüher M, Klötting N. Fat depot-specific expression of HOXC9 and HOXC10 may contribute to adverse fat distribution and related metabolic traits. *Obesity (Silver Spring)* 24: 51–59, 2016. doi:10.1002/oby.21317.
- Brunet P, Gondouin B, Duval-Sabatier A, Dou L, Cerini C, Dignat-George F, Jourde-Chiche N, Argiles A, Burtsey S. Does uremia cause vascular dysfunction? *Kidney Blood Press Res* 34: 284–290, 2011. doi:10.1159/000327131.
- Carbó C, Arderiu G, Escobar G, Fusté B, Cases A, Carrascal M, Abián J, Díaz-Ricart M. Differential expression of proteins from cultured endothelial cells exposed to uremic versus normal serum. *Am J Kidney Dis* 51: 603–612, 2008. doi:10.1053/j.ajkd.2007.11.029.
- Cowburn AS, Takeda N, Boutin AT, Kim JW, Sterling JC, Nakasaki M, Southwood M, Goldrath AW, Jamora C, Nizet V, Chilvers ER, Johnson RS. HIF isoforms in the skin differentially regulate systemic arterial pressure. *Proc Natl Acad Sci USA* 110: 17570–17575, 2013. doi:10.1073/pnas.1306942110.
- Dahlquist KD, Salomonis N, Vranizan K, Lawlor SC, Conklin BR. GenMAPP, a new tool for viewing and analyzing microarray data on biological pathways. *Nat Genet* 31: 19–20, 2002. doi:10.1038/ng0502-19.
- Dai X, Zeng Z, Fu C, Zhang S, Cai Y, Chen Z. Diagnostic value of neutrophil gelatinase-associated lipocalin, cystatin C, and soluble triggering receptor expressed on myeloid cells-1 in critically ill patients with sepsis-associated acute kidney injury. *Crit Care* 19: 223, 2015. doi:10.1186/s13054-015-0941-6.
- Dinardo CL, Venturini G, Zhou EH, Watanabe IS, Campos LC, Dariolli R, da Motta-Leal-Filho JM, Carvalho VM, Cardozo KH, Krieger JE, Alencar AM, Pereira AC. Variation of mechanical properties and quantitative proteomics of VSMC along the arterial tree. *Am J Physiol Heart Circ Physiol* 306: H505–H516, 2014. doi:10.1152/ajpheart.00655.2013.
- Doniger SW, Salomonis N, Dahlquist KD, Vranizan K, Lawlor SC, Conklin BR. MAPPFinder: using Gene Ontology and GenMAPP to create a global gene-expression profile from microarray data. *Genome Biol* 4: R7, 2003. doi:10.1186/gb-2003-4-1-r7.
- Feng B, Zhang Y, Mu J, Ye Z, Zeng W, Qi W, Luo Z, Guo Y, Yang X, Yuan F. Preventive effect of a proteasome inhibitor on the formation of accelerated atherosclerosis in rabbits with uremia. *J Cardiovasc Pharmacol* 55: 129–138, 2010. doi:10.1097/FJC.0b013e3181c87f8e.
- Foley RN, Murray AM, Li S, Herzog CA, McBean AM, Eggers PW, Collins AJ. Chronic kidney disease and the risk for cardiovascular disease, renal replacement, and death in the United States Medicare population, 1998 to 1999. *J Am Soc Nephrol* 16: 489–495, 2005. doi:10.1681/ASN.2004030203.
- Goligorsky MS, Yasuda K, Ratliff B. Dysfunctional endothelial progenitor cells in chronic kidney disease. *J Am Soc Nephrol* 21: 911–919, 2010. doi:10.1681/ASN.2009111119.
- Goodman WG, Goldin J, Kuizon BD, Yoon C, Gales B, Sider D, Wang Y, Chung J, Emerick A, Greaser L, Elashoff RM, Salusky IB. Coronary-artery calcification in young adults with end-stage renal disease who are undergoing dialysis. *N Engl J Med* 342: 1478–1483, 2000. doi:10.1056/NEJM200005183422003.
- Hakuno D, Kimura N, Yoshioka M, Mukai M, Kimura T, Okada Y, Yozu R, Shukunami C, Hiraki Y, Kudo A, Ogawa S, Fukuda K. Periostin advances atherosclerotic and rheumatic cardiac valve degeneration by inducing angiogenesis and MMP production in humans and rodents. *J Clin Invest* 120: 2292–2306, 2010. doi:10.1172/JCI40973.
- Heikkilä M, Pasanen A, Kivirikko KI, Myllyharju J. Roles of the human hypoxia-inducible factor (HIF)-3 α variants in the hypoxia response. *Cell Mol Life Sci* 68: 3885–3901, 2011. doi:10.1007/s00018-011-0679-5.
- Ignat M, Teletin M, Tisserand J, Khetchoumian K, Dennefeld C, Chambon P, Losson R, Mark M. Arterial calcifications and increased expression of vitamin D receptor targets in mice lacking TIF1 α . *Proc Natl Acad Sci USA* 105: 2598–2603, 2008. doi:10.1073/pnas.0712030105.

20. Ihaka R, Gentleman R. R: a language for data analysis and graphics. *J Comp Graph Stat* 5: 299–314, 1996. doi:10.1080/10618600.1996.10474713.
21. Irizarry RA, Hobbs B, Collin F, Beazer-Barclay YD, Antonellis KJ, Scherf U, Speed TP. Exploration, normalization, and summaries of high density oligonucleotide array probe level data. *Biostatistics* 4: 249–264, 2003. doi:10.1093/biostatistics/4.2.249.
22. Kashani K, Al-Khafaji A, Ardiles T, Artigas A, Bagshaw SM, Bell M, Bihorac A, Birkhahn R, Cely CM, Chawla LS, Davison DL, Feldkamp T, Forni LG, Gong MN, Gunnerson KJ, Haase M, Hackett J, Honore PM, Hoste EA, Joannes-Boyau O, Joannidis M, Kim P, Koyner JL, Laskowitz DT, Lissauer ME, Marx G, McCullough PA, Mullaney S, Ostermann M, Rimmelé T, Shapiro NI, Shaw AD, Shi J, Sprague AM, Vincent JL, Vinsonneau C, Wagner L, Walker MG, Wilkerson RG, Zacharowski K, Kellum JA. Discovery and validation of cell cycle arrest biomarkers in human acute kidney injury. *Crit Care* 17: R25, 2013. doi:10.1186/cc12503.
23. Kelly RP, Tunin R, Kass DA. Effect of reduced aortic compliance on cardiac efficiency and contractile function of in situ canine left ventricle. *Circ Res* 71: 490–502, 1992. doi:10.1161/01.RES.71.3.490.
24. Koyama A, Fujita T, Gejyo F, Origasa H, Isono M, Kurumatani H, Okada K, Kanoh H, Kiriyama T, Yamada S. Orally active prostacyclin analogue beraprost sodium in patients with chronic kidney disease: a randomized, double-blind, placebo-controlled, phase II dose finding trial. *BMC Nephrol* 16: 165, 2015. doi:10.1186/s12882-015-0130-5.
25. Lee HK, Deneen B. Daam2 is required for dorsal patterning via modulation of canonical Wnt signaling in the developing spinal cord. *Dev Cell* 22: 183–196, 2012. doi:10.1016/j.devcel.2011.10.025.
26. Lee SH, Youn YN, Choo HC, Lee S, Yoo KJ. Cystatin C as a predictive marker of renal dysfunction and mid-term outcomes following off-pump coronary artery bypass grafting. *Heart* 101: 1562–1568, 2015. doi:10.1136/heartjnl-2015-307986.
27. Li G, Jin R, Norris RA, Zhang L, Yu S, Wu F, Markwald RR, Nanda A, Conway SJ, Smyth SS, Granger DN. Periostin mediates vascular smooth muscle cell migration through the integrins α 5 β 3 and α 5 β 1 and focal adhesion kinase (FAK) pathway. *Atherosclerosis* 208: 358–365, 2010. doi:10.1016/j.atherosclerosis.2009.07.046.
28. Lian N, Lin T, Liu W, Wang W, Li L, Sun S, Nyman JS, Yang X. Transforming growth factor β suppresses osteoblast differentiation via the vimentin activating transcription factor 4 (ATF4) axis. *J Biol Chem* 287: 35975–35984, 2012. doi:10.1074/jbc.M112.372458.
29. Lin ME, Chen T, Leaf EM, Speer MY, Giachelli CM. Runx2 Expression in Smooth Muscle Cells Is Required for Arterial Medial Calcification in Mice. *Am J Pathol* 185: 1958–1969, 2015. doi:10.1016/j.ajpath.2015.03.020.
30. Lindner A, Charra B, Sherrard DJ, Scribner BH. Accelerated atherosclerosis in prolonged maintenance hemodialysis. *N Engl J Med* 290: 697–701, 1974. doi:10.1056/NEJM197403282901301.
31. Liu F, Fu P, Fan W, Gou R, Huang Y, Qiu H, Zhong H, Huang S. Involvement of parathyroid hormone-related protein in vascular calcification of chronic haemodialysis patients. *Nephrology (Carlton)* 17: 552–560, 2012. doi:10.1111/j.1440-1797.2012.01601.x.
32. McDougall AR, Tolcos M, Hooper SB, Cole TJ, Wallace MJ. Trop2: from development to disease. *Dev Dyn* 244: 99–109, 2015. doi:10.1002/dvdy.24242.
33. Neven E, Persy V, Dauwe S, De Schutter T, De Broe ME, D'Haese PC. Chondrocyte rather than osteoblast conversion of vascular cells underlies medial calcification in uremic rats. *Arterioscler Thromb Vasc Biol* 30: 1741–1750, 2010. doi:10.1161/ATVBAHA.110.204834.
34. Niederhoffer N, Lartaud-Idjouadiene I, Giummelly P, Duvivier C, Peslin R, Atkinson J. Calcification of medial elastic fibers and aortic elasticity. *Hypertension* 29: 999–1006, 1997. doi:10.1161/01.HYP.29.4.999.
35. Ostrowska JK, Wojtukiewicz MZ, Chabielska E, Buczek W, Ostrowska H. Proteasome inhibitor prevents experimental arterial thrombosis in renovascular hypertensive rats. *Thromb Haemost* 92: 171–177, 2004. doi:10.1160/TH03-11-0707.
36. Owens GK, Kumar MS, Wamhoff BR. Molecular regulation of vascular smooth muscle cell differentiation in development and disease. *Physiol Rev* 84: 767–801, 2004. doi:10.1152/physrev.00041.2003.
37. Pai A, Leaf EM, El-Abbadi M, Giachelli CM. Elastin degradation and vascular smooth muscle cell phenotype change precede cell loss and arterial medial calcification in a uremic mouse model of chronic kidney disease. *Am J Pathol* 178: 764–773, 2011. doi:10.1016/j.ajpath.2010.10.006.
38. Pen A, Durocher Y, Slinn J, Rukhlova M, Charlebois C, Stanimirovic DB, Moreno MJ. Insulin-like growth factor binding protein 7 exhibits tumor suppressive and vessel stabilization properties in U87MG and T98G glioblastoma cell lines. *Cancer Biol Ther* 12: 634–646, 2011. doi:10.4161/cbt.12.7.17171.
39. Poitz DM, Augstein A, Weinert S, Braun-Dullaues RC, Strasser RH, Schmeisser A. OxLDL and macrophage survival: essential and oxygen-independent involvement of the Hif-pathway. *Basic Res Cardiol* 106: 761–772, 2011. doi:10.1007/s00395-011-0186-8.
40. Preil SA, Kristensen LP, Beck HC, Jensen PS, Nielsen PS, Steiniche T, Björling-Poulsen M, Larsen MR, Hansen ML, Rasmussen LM. Quantitative proteome analysis reveals increased content of basement membrane proteins in arteries from patients with type 2 diabetes mellitus and lower levels among metformin users. *Circ Cardiovasc Genet* 8: 727–735, 2015. doi:10.1161/CIRCGENETICS.115.001165.
41. Price SR, Reaich D, Marinovic AC, England BK, Bailey JL, Caban R, Mitch WE, Maroni BJ. Mechanisms contributing to muscle-wasting in acute uremia: activation of amino acid catabolism. *J Am Soc Nephrol* 9: 439–443, 1998.
42. Proudfoot D, Skepper JN, Hegyi L, Bennett MR, Shanahan CM, Weissberg PL. Apoptosis regulates human vascular calcification in vitro: evidence for initiation of vascular calcification by apoptotic bodies. *Circ Res* 87: 1055–1062, 2000. doi:10.1161/01.RES.87.11.1055.
43. Rukov JL, Gravesen E, Mace ML, Hofman-Bang J, Vinther J, Andersen CB, Lewin E, Olgaard K. Effect of chronic uremia on the transcriptional profile of the calcified aorta analyzed by RNA sequencing. *Am J Physiol Renal Physiol* 310: F477–F491, 2016. doi:10.1152/ajprenal.00472.2015.
44. Schlosser A, Pilecki B, Hemstra LE, Keijling K, Kristmannsdottir GB, Wulf-Johansson H, Moeller JB, Füchtbauer EM, Nielsen O, Kirketerp-Møller K, Dubey LK, Hansen PB, Stubbe J, Wrede C, Hegermann J, Ochs M, Rathkolb B, Schrewe A, Bekeredjian R, Wolf E, Gailus-Durner V, Fuchs H, Hrabě de Angelis M, Lindholt JS, Holmskov U, Sorensen GL. MFAP4 promotes vascular smooth muscle migration, proliferation and accelerates neointima formation. *Arterioscler Thromb Vasc Biol* 36: 122–133, 2016. doi:10.1161/ATVBAHA.115.306672.
45. Schwarz U, Buzello M, Ritz E, Stein G, Raabe G, Wiest G, Mall G, Amann K. Morphology of coronary atherosclerotic lesions in patients with end-stage renal failure. *Nephrol Dial Transplant* 15: 218–223, 2000. doi:10.1093/ndt/15.2.218.
46. Seijffers R, Mills CD, Woolf CJ. ATF3 increases the intrinsic growth state of DRG neurons to enhance peripheral nerve regeneration. *J Neurosci* 27: 7911–7920, 2007. doi:10.1523/JNEUROSCI.5313-06.2007.
47. Shroff RC, McNair R, Skepper JN, Figg N, Schurgers LJ, Deanfield J, Rees L, Shanahan CM. Chronic mineral dysregulation promotes vascular smooth muscle cell adaptation and extracellular matrix calcification. *J Am Soc Nephrol* 21: 103–112, 2010. doi:10.1681/ASN.2009060640.
48. Skene JH, Virág I. Posttranslational membrane attachment and dynamic fatty acylation of a neuronal growth cone protein, GAP-43. *J Cell Biol* 108: 613–624, 1989. doi:10.1083/jcb.108.2.613.
49. Skov V, Glinthorg D, Knudsen S, Jensen T, Kruse TA, Tan Q, Brusgaard K, Beck-Nielsen H, Højlund K. Reduced expression of nuclear-encoded genes involved in mitochondrial oxidative metabolism in skeletal muscle of insulin-resistant women with polycystic ovary syndrome. *Diabetes* 56: 2349–2355, 2007. doi:10.2337/db07-0275.
50. Smyth GK. Linear models and empirical bayes methods for assessing differential expression in microarray experiments. *Stat Appl Genet Mol Biol* 3: e3, 2004. doi:10.2202/1544-6115.1027.
51. Speer MY, Yang HY, Brabb T, Leaf E, Look A, Lin WL, Frutkin A, Dichek D, Giachelli CM. Smooth muscle cells give rise to osteochondrogenic precursors and chondrocytes in calcifying arteries. *Circ Res* 104: 733–741, 2009. doi:10.1161/CIRCRESAHA.108.183053.
52. Svensson L, Aszódi A, Reinholt PP, Fässler R, Heinegård D, Oldberg A. Fibromodulin-null mice have abnormal collagen fibrils, tissue organization, and altered lumican deposition in tendon. *J Biol Chem* 274: 9636–9647, 1999. doi:10.1074/jbc.274.14.9636.
53. Takeda N, O'Dea EL, Doedens A, Kim JW, Weidemann A, Stockmann C, Asagiri M, Simon MC, Hoffmann A, Johnson RS. Differential activation and antagonistic function of HIF- α isoforms in macrophages are essential for NO homeostasis. *Genes Dev* 24: 491–501, 2010. doi:10.1101/gad.188140.

54. Vattikuti R, Towler DA. Osteogenic regulation of vascular calcification: an early perspective. *Am J Physiol Endocrinol Metab* 286: E686–E696, 2004. doi:[10.1152/ajpendo.00552.2003](https://doi.org/10.1152/ajpendo.00552.2003).
55. Vogel C, Marcotte EM. Insights into the regulation of protein abundance from proteomic and transcriptomic analyses. *Nat Rev Genet* 13: 227–232, 2012. doi:[10.1038/nrg3185](https://doi.org/10.1038/nrg3185).
56. Yamaguchi S, Inada C, Tamura M, Sato N, Yamada M, Itaba S, Okazaki S, Matsuura H, Fujii S, Matsuda F, Goto Y, Mochizuki H, Kurumatani H, Miyamoto M. Beraprost sodium improves survival rates in anti-glomerular basement membrane glomerulonephritis and 5/6 nephrectomized chronic kidney disease rats. *Eur J Pharmacol* 714: 325–331, 2013. doi:[10.1016/j.ejphar.2013.07.032](https://doi.org/10.1016/j.ejphar.2013.07.032).
57. Yao W, Sun Q, Huang L, Meng G, Wang H, Jing X, Zhang W. Tetrahydroxystilbene glucoside inhibits TNF- α -induced migration of vascular smooth muscle cells via suppression of vimentin. *Can J Physiol Pharmacol*: 1–6, 2015. doi:[10.1139/cjpp-2015-0160](https://doi.org/10.1139/cjpp-2015-0160).
58. Zhang YQ, Feng B, Yuan FH. Effect of chronic renal failure medium on the ubiquitin-proteasome pathway of arterial muscle cells. *Mol Med Rep* 7: 1021–1025, 2013. doi:[10.3892/mmr.2013.1269](https://doi.org/10.3892/mmr.2013.1269).
59. Aarhi JJ, Darendeliler MA, Pushparaj PN. Dissecting the role of the S1P/S1PR axis in health and disease. *J Dent Res* 90: 841–854, 2011. doi:[10.1177/0022034510389178](https://doi.org/10.1177/0022034510389178).
60. Aarup A, Pedersen TX, Junker N, Christoffersen C, Bartels ED, Madsen M, Nielsen CH, Nielsen LB. Hypoxia-Inducible Factor-1 α Expression in Macrophages Promotes Development of Atherosclerosis. *Arterioscler Thromb Vasc Biol* 36: 1782–1790, 2016. doi:[10.1161/ATVBAHA.116.307830](https://doi.org/10.1161/ATVBAHA.116.307830).

